

Ab Initio Structure Solution from X-ray Powder Data at Moderate Resolution: Crystal Structure of a Microporous Layer Silicate

Silke Vortmann,[†] Jordi Rius,[‡] Silvester Siegmann,[†] and Hermann Gies^{*,†}

Institut für Mineralogie, Ruhr-Universität Bochum, 47800 Bochum, Germany, and Institut de Ciencia de Materials de Barcelona, 08193 Bellaterra, Catalunya, Spain

Received: July 17, 1996; In Final Form: November 15, 1996[Ⓢ]

The ab initio crystal structure solution of a layer silicate is presented. Since the crystallinity of the material is limited, the corresponding X-ray powder pattern shows only moderate resolution. Based on a new interpretation of the tangent formula, a general direct method strategy for the determination of the crystal structure of poorly crystalline materials from X-ray powder patterns is presented. The structure model derived from the interpretation of the *E* map was subsequently refined with the Rietveld technique using the whole diffraction pattern. This leads finally to a picture of the crystal structure of atomic resolution which explains in full detail the specific characteristics of the material.

Introduction

Microporous silicates are characteristically open framework structures built from tetrahedral [SiO₄] units and contain internal cavities that are accessible through one-, two-, or three-dimensional pore systems. These channels are in the range of molecular dimensions and remain open even after removal of the pore-filling nonframework constituents. The rigid silicate frame serves as a backbone for the solid and gives the structures their molecular sieving characteristics. Because of this chemical selectivity, they are widely used as sorbents, catalysts, and ion exchangers, particularly in the washing powder industry. Apart from framework structures, layered microporous silicates have attracted much interest for industrial applications because of their cheap manufacture, their potential in modification of properties through pillaring, and their high ion exchange selectivity and capacity.¹ As in zeolite frameworks, the properties depend on the accessibility of the internal surface of the material which is in general crystalline. The internal surface is part of the regular crystal structure and does not suffer from structural and electronic distortion effects known from external surfaces. The knowledge of the crystal structure, therefore, is the key to the understanding of the physical and chemical properties of the family of microporous materials. It also serves for extrapolating properties and for the theoretical simulation processes involving microporous heterogeneous catalysts.

In general, the zeolite framework materials are highly crystalline, but they are almost always microcrystalline with particle size on the order of microns. This precludes single-crystal X-ray diffraction experiments, and recourse must be made to much more limited powder diffraction experiments. In the case of layered microporous silicates the crystallinity of the material is very often inferior, restricting diffraction information to *d* values in the range 2–1.5 Å; thus, the limiting factor in the diffraction experiment is not the instrumental resolution but the reduced crystallinity of the material. Although in the past several techniques have been developed for the solution of crystal structures from X-ray and neutron powder data, they all require diffraction information close to atomic resolution, with the integrated intensities of reflections up to *d* values of 1 Å, inevitably failing with low-resolution intensity data sets. The

only method not requiring atomic resolution, direct interpretation of the Patterson function, is of little help because (a) microporous materials consists of light elements only and (b) the metal cations, if present, tend to be severely disordered. Other alternatives such as the application of Patterson search techniques, although viable,^{2,3} are far from trivial. Finally, theoretical approaches such as simulated annealing of trial structures are all restricted to a well-predefined set of rules describing the potential structure and are, therefore, not of general use.

In previous work, Rius and co-workers^{4,5} have introduced a new physical interpretation of direct methods based on the Patterson function and on the fulfillment of the atomicity condition. This new concept allows derivation of a more robust phase refinement function which leads to the sum function tangent formula (SUMF-TF) which has been found to be very effective in solving difficult structures. Unfortunately, when working with intensity data extracted from powder patterns of zeolites or layered microporous silicates, the atomicity condition is in general not satisfied, so that direct methods should in principle not be applicable. However, if one considers the structural unit of the framework, i.e., the [SiO₄] tetrahedron, as a single dominant scatterer, then the “atomicity” condition is satisfied even with intensity data at moderate resolution. This means that direct methods can be applied to reveal the positions of the centers of the tetrahedra provided that the selected direct method procedure is powerful enough. Once the centers are known, the silicate bonding network is obvious.

In this paper we describe the structure solution of a layered microporous Na–silicate material (code name RUB-18) and demonstrate that the silicate bonding network can be effectively obtained applying the SUMF-TF to moderate-resolution intensity data. The rest of the structure and the hydrogen bond system were determined by Fourier methods during the course of the subsequent Rietveld analysis.

Experimental Section

Material. RUB-18 was synthesized in the system SiO₂/Na₂O/Cs₂O/hexamethylenetetramine/triethanolamine/H₂O in Teflon line steel autoclaves at 95 °C. The autoclaves were kept for 21–28 days without stirring in an oven. The material was recovered in pure form by filtering and washing the crystalline phase with ethanol and water. The scanning electron microscope images show that the microcrystals are very thin platelets

[†] Institut für Mineralogie.

[‡] Institut de Ciencia de Materials de Barcelona.

[Ⓢ] Abstract published in *Advance ACS Abstracts*, January 15, 1997.

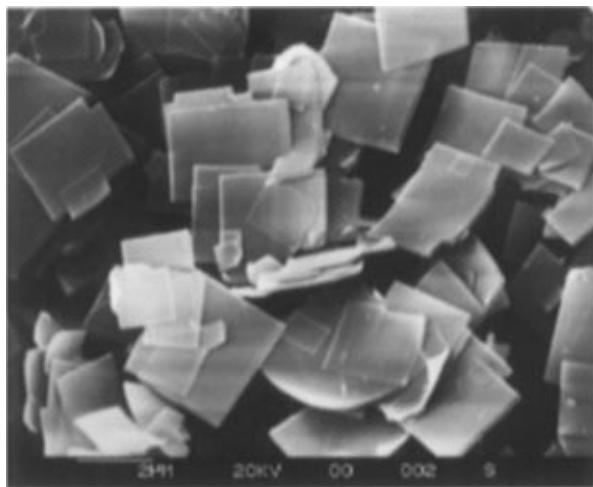


Figure 1. Scanning electron micrograph of the layer silicate RUB-18 showing crystals with platelike morphology.

(<0.1 μm) with orthogonal edges in the other two dimensions of 1–2 μm (Figure 1). The ratio of Si:Na:H₂O was obtained from chemical analysis. Thermal analysis was conducted on a Linseis (Type 20456) thermal analyzer from room temperature to 1250 °C and 10 °C/min heating rate. Thermogravimetry and DTA experiments show a weight loss of 20% in the range 100–200 °C in two steps indicated by two endothermic DTA signals, which corresponds to 32 water molecules per unit cell. At ca. 700 °C an exothermic event reveals the transformation of the dehydrated RUB-18 material to tridymite. High-temperature X-ray studies in the range 100–800 °C confirm this results. The weight loss in the TGA experiment is in agreement with the amount of water determined with Karl Fischer titration (19.5%).

NMR Experiments. ²⁹Si and ²³Na MAS NMR experiments were performed on a Bruker ASX-400 spectrometer with single-pulse experiments. The ²⁹Si MAS NMR spectrum gives one signal at –100 ppm from TMS for Q³ silicon connected to three [SiO₄] tetrahedra and one OH group and another signal at –111 ppm for Q⁴ silicon connected only to [SiO₄] tetrahedra (Figure 2a). The intensity ratio of the two signals is 1:1, indicating that there is a layered polysilicate anion containing one Q⁴ unit per Q³ unit. This is in agreement with the platelike morphology and the perfect cleavage in {001} of the particles. ²³Na MAS NMR (Figure 2b) shows one rather narrow signal at 1.4 ppm from NaCl (fwhm 150 Hz) typical for a geometrically regular coordination polyhedron, most likely an octahedron.

X-ray Powder Diffraction. The powder pattern was collected on a Siemens D-5000 diffractometer in a modified Debye–Scherrer geometry, using monochromated Cu K α_1 radiation ($\lambda = 1.54059 \text{ \AA}$) and a capillary sample holder. The intensity data were recorded in the range 6–75° 2 θ . Crystal data and relevant details of data collection are summarized in Table 1. The powder diagram was indexed in the tetragonal system using the program TREOR.⁶ A total of 138 integrated intensities up to 2 $\theta = 62^\circ$ ($d_{\text{min}} = 1.5 \text{ \AA}$) were extracted from the powder pattern with the program AJUST.⁷ The space group was derived, without ambiguity, from the observed systematic extinctions. The available integrated intensities were introduced in the direct methods program XLENS.⁸ The number of large and weak *E* values actively used are 45 and 40, respectively. The starting framework model was derived from the interpretation of the electron density map computed with the set of refined phases with the highest combined figure of merit. This model was optimized with a distance least-squares program, DLS,⁹ using the distances $d(\text{Si–O}) = 1.60(1) \text{ \AA}$ as restraints. Preliminary refinements and location of the missing atoms were

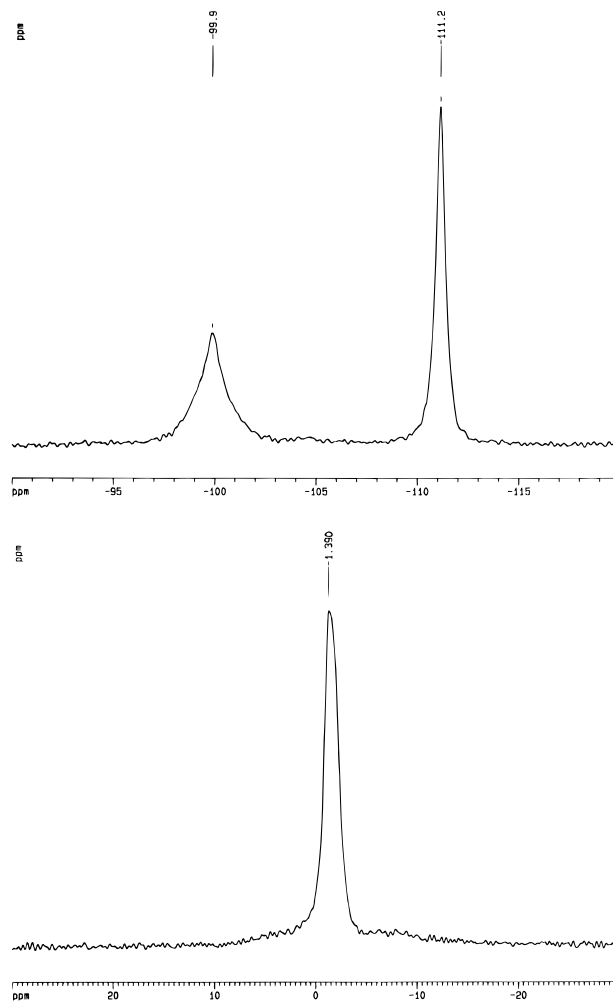


Figure 2. (a, top) ²⁹Si MAS NMR spectrum consists of two signals due to Q³ and Q⁴ units, i.e., [Si(3Si, 1OH)] and [Si(4Si)], respectively. The intensity ratio of 1:1 indicates a layered crystal structure. (b, bottom) ²³Na MAS NMR spectrum shows only one narrow signal typical for a geometrically regular coordination of the sodium cations.

TABLE 1: Analytical Results from Chemical Analysis, X-ray Diffraction, and NMR Spectroscopy

Chemical Analysis	
Si (ICP experiment)	28.8 wt %
Na (ICP experiment)	8.6 wt %
H ₂ O (Karl–Fischer titration)	19.95 wt %
DTA Experiments	
weight loss in the range 100–200 °C	20 wt % in two steps
transformation at ca. 700 °C to	tridymite
NMR Experiments	
²⁹ Si MAS NMR (standard TMS)	–100 ppm (Q ³ : [Si(3Si, 1OH)])
	–111 ppm (Q ⁴ : [Si(4Si)])
²³ Na MAS NMR (standard NaCl)	1.4 ppm
Unit Cell	
<i>a</i> ₀	7.3276(1) Å
<i>c</i> ₀	44.3191(6) Å
space group	<i>I</i> 4 ₁ / <i>amd</i> (choice 2)
cell content	Na[Si ₄ O ₈ (OH)]·4H ₂ O
	<i>Z</i> = 8

done with SHELXTL¹⁰ using the integrated intensities. Once the structure was complete, the full pattern Rietveld analysis was performed with the program system XRS-82¹¹ employing the entire powder data set.

Structure Solution

Nowadays, the solution of small- and medium-sized crystal structures from single-crystal data is in most cases a routine

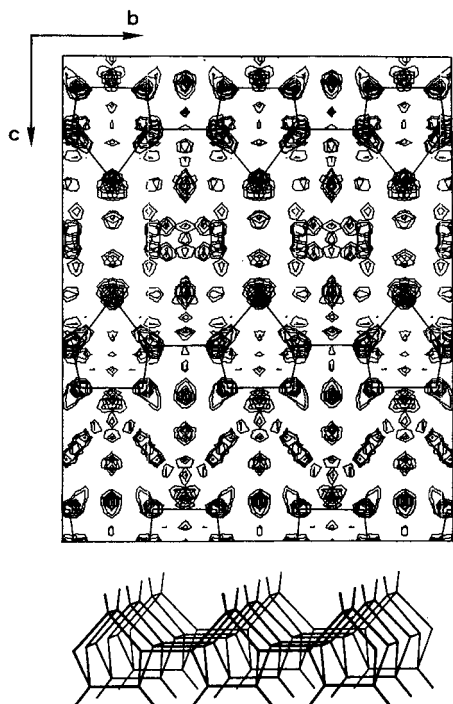


Figure 3. (a, top) The (100) projection of the electron density map obtained from direct methods. The silicon atoms appear as clearly resolved peaks. The narrow lines connecting the Si atoms correspond to the silicate layer model represented in (b, bottom). The absence of the bonding oxygen atoms in the middle of the Si...Si bonds is a consequence of the moderate resolution of the intensity data set processed with the SUM-TF.

process. In contrast, solving structures from powder data is very often a challenging task. This is principally due to the presence of peak overlap which reduces the number of unambiguously indexed reflections and hence the effective

resolution of the intensity data set available for direct methods. In general, the application of direct methods to powder data can be divided into three stages:

(a) *Extraction of Enough Integrated Intensities from the Powder Pattern.* Modern extraction procedures obtain the integrated intensities applying whole-pattern fitting methods which use the metric and the space group symmetry as constraints. This philosophy was first introduced by Pawley.¹² However, it is the more simple two-stage procedure of LeBail et al.¹³ which is being increasingly used. Unlike Pawley's method, the latter refines the integrated intensities and the profile parameters separately. The integrated intensities are estimated applying iteratively the formula

$$I(\mathbf{k})_{\text{new}} = I(\mathbf{k})_{\text{old}} \sum_i \Omega(\mathbf{k}, i) [y_o(i)/y_c(i)] \quad (1)$$

where the summation extends over the i points of the pattern for which the value of the profile function Ω of reflection \mathbf{k} is not negligible, and where $y_o(i)$ and $y_c(i)$ are respectively the net observed and calculated counts at $2\theta(i)$. This method tolerates large errors in the initial estimates of the integrated intensities although some troubles may arise when the denominator becomes zero. Recently, Rius et al.¹⁴ have derived an alternative expression for refining iteratively integrated intensities. This new recursive formula, which has been used to extract the integrated intensities employed for solving RUB-18, is

$$I(\mathbf{k})_{\text{new}} = I(\mathbf{k})_{\text{old}} + c(\mathbf{k}) \sum_i w(i) \Omega(\mathbf{k}, i) [y_o(i) - y_c(i)] \quad (2)$$

$$c(\mathbf{k}) = 1 / \sum_i w(i) \Omega(\mathbf{k}, i)^2 \quad (3)$$

where the quotient present in (1) has been replaced by a difference in (2). Expression 2 furnishes reliable integrated

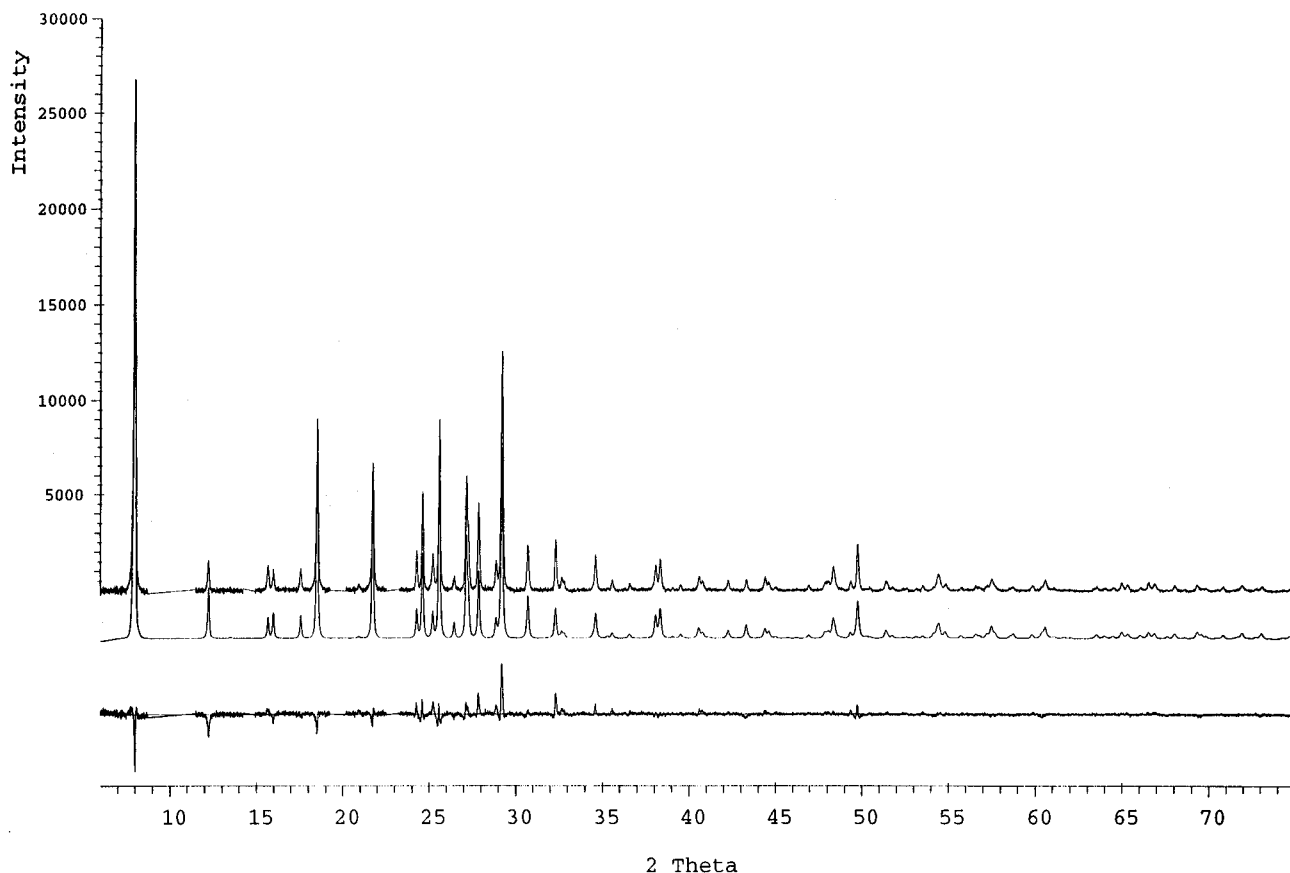


Figure 4. Observed (top) and calculated (middle) X-ray powder pattern of RUB-18 and difference profile (bottom) from Rietveld refinement.

intensities if the angular distances to the closest neighboring reflections are greater than the half-width at half-maximum even when all initial estimates $I(\mathbf{k})_{\text{old}}$ are zero. When the accidental peak overlap is severe, one can estimate, in favorable cases, the corresponding integrated intensities by different techniques, for example using the maximum entropy algorithm,¹⁵ the fast iterative Patterson squaring method,¹⁶ or also the relations between structure factors.¹⁷

(b) *Application of Low-Resolution Direct Methods.* Due to the severe peak overlap observed in the powder patterns of many layered microporous materials, the effective resolution of the set of reflections with reliable integrated intensities is considerably reduced when compared to single-crystal data. This limited resolution precludes direct methods to be used indiscriminately with powder data. Recently, it has been shown⁵ that the required data resolution for applying direct methods largely depends on the closest separation s_D between dominant scatterers in the structure, suggesting that for a given s_D the required intensity data resolution expressed in terms of the minimum d spacing is given by

$$d_{\min} = s_D/1.44 \quad (4)$$

Obviously, the corresponding direct methods solution will principally reveal the partial structure of the dominant scatterers. The two cases represented by the organic (only C, N, and O atoms) and the zeolitic compounds are very illustrative. While in organic structures, a d_{\min} value of 1 Å ($s_D = 1.45$ Å) is required, in zeolitic compounds, where the $[\text{SiO}_4]$ tetrahedra act to some extent as dominant scatterers, d_{\min} values of the order of 2 Å can be tolerated as the minimum separation between the Si atoms is approximately 3.1 Å. An additional difficulty which is normally found in practice is that the set of low-resolution intensity data is incomplete. This demands a robust and effective direct method procedure as for example the sum function defined by the integral

$$V \int_{\Phi} P'_{\Phi}(\mathbf{u}) P(\mathbf{u}, \Phi) d\mathbf{u} \quad (5)$$

which measures the coincidence of the observed Patterson-type function P'_{Φ} without origin peak with the calculated one $P(\Phi)$ expressed in terms of the collectivity Φ of phases of the reflections with large structure factor magnitudes. In the calculation of $P(\Phi)$, both the atomicity condition and the known magnitudes of the structure factors are introduced as restrictions. Obviously, for a good coincidence between observed and calculated nonorigin Patterson peaks, the integral must be large. Rius⁴ showed that it can be maximized by an extended tangent formula (SUMF-TF) which constitutes the heart of the direct method program XLENS. Two unique features of this tangent formula are that it uses the same number of large and small structure factors, thus allowing the use of a large number of extracted intensities in the phase refinement and that the small ones need not be introduced by any weighting function. This gives to the SUMF-TF an increased stability which allows it to work in precarious conditions.

(c) *Interpretation of the Low-Resolution Fourier Map.* When using intensity data up to low or moderate resolution (that is, for d_{\min} values in the range 2–1.5 Å), the $[\text{SiO}_4]$ units appear as isolated maxima in the Fourier map computed with the phases supplied by direct methods. Figure 3a illustrates this for RUB-18. For clarity, the skeleton model of the silicate layer (Figure 3b) has been outlined in the (100) projection of the unit cell. In the structure, the interlayer separation is given by the 4_1 screw axis. The interpretation of the Fourier maxima was greatly facilitated by the information provided by the ^{29}Si MAS NMR spectrum which indicates that the silicate layer contains Q^3 and

TABLE 2: Results of the Rietveld Refinement of RUB-18

X-ray Diffraction	
wavelength, Å	1.54059
profile range, deg (2θ)	6–75
step size, deg (2θ)	0.007758
Refinement	
peak range in fwhm	15.0
number of data points	8231
number of contributing reflections	188
number of profile parameters	5
number of structural parameters	19
number of structural restraints	5
Geometric Restraints	
$d(\text{Si}-\text{O})$, Å	1.60(1)
Residuals	
$R_I = \sum_i I(\text{obs}) - I(\text{calc}) / \sum_i I(\text{obs})$	0.127
$R_F = \sum_i F(\text{obs}) - F(\text{calc}) / \sum_i F(\text{obs})$	0.080
$R_{\text{wp}} = \{ \sum_i w_i [y_i(\text{obs}) - y_i(\text{calc})]^2 / \sum_i w_i y_i^2(\text{obs}) \}^{1/2}$	0.167
$R_{\text{exp}} = [(N - P) / \sum_i w_i y_i^2(\text{obs})]^{1/2}$	0.146
weighting scheme	$1/\sigma(Y)$
common weight factor for soft restrictions	3

TABLE 3: Fractional Coordinates and Equivalent Temperature Parameters (Å²) for RUB-18

atom ^a	Wyckhoff letter	x	y	z	B_{eq}
Si1	16 g	0.289(1)	0.039(1)	1/8	1.5
Si2	16 h	0	0.544(1)	0.074(1)	1.5
O1	32 i	0.171(1)	0.987(1)	0.096(1)	3.1
O2	16 h	0.253(1)	1/4	0.134(1)	3.1
O3	8 e	0	3/4	0.062(1)	3.1
O4	16 h	0	0.093(1)	0.045(1)	3.5
Na	8 e	1/2	1/4	0.002(1)	6.0
O5	16 f	0.254(1)	1/2	0	4.0
O6	8 e	1/2	3/4	0.053(1)	4.0
O7	8 e	1/2	1/4	0.051(1)	4.0

^a O5, O6, and O7 are the water molecules.

Q^4 silicon atoms in a 1:1 ratio. The Fourier map also shows peaks between the silicate layers. The strongest ones were initially assigned to the sodium atoms. However, the refinement indicated that these peaks are in fact water molecules. Due to their higher displacement parameters, which becomes obvious in subsequent stages of the refinement, the peaks of the sodium atoms do not appear in the first Fourier map. The mobility of the cations and consequently the microporous character of RUB-18 are confirmed by the ion exchange capability of layered silicates.¹ The next step was to optimize the approximate geometry of the silicate layer by a DLS refinement using the Si–O distances of 1.6 Å as restraints. To complete the structure, the DLS model was introduced in a single-crystal refinement program. The refinement was performed with the integrated intensities already used in the structure solution processes and with the geometry of the optimized layer kept fixed ($B_{\text{over}} = 3$ Å²). Inspection of the subsequent ΔF synthesis revealed the positions of the sodium cation and of the two missing symmetry-independent water molecules forming the sodium coordination polyhedron. To increase the accuracy of the atomic positions, a restrained Rietveld refinement now exploiting the scattering information up to $2\theta = 75^\circ$ ($d_{\min} = 1.27$ Å) was performed (Figure 4). The refinement of the full pattern provides nearly atomic resolution with highly reliable positional parameters including the hydrogen bridge bonding network of the silanol group of the silicate layer and the intercalated water molecules. A full account of the structure refinement is summarized in Table 2. Fractional coordinates of the refined structure of RUB-18 are presented in Table 3; selected angles and distances are given in Table 4. A perspective view of the crystal structure is shown in Figure 5, and the atom numbering is indicated in Figure 6.

TABLE 4: Selected Bond Distances (Å) for RUB-18 (Esd's in Parentheses)

Si1...Si1	3.098(1)	Na—O5	2.570(4) (4×)
Si1...Si2	3.167(2)	Na—O6	2.25(1)
Si1—O1	1.586(3) (2×)	Na—O7	2.34(1)
Si1—O2	1.618(2) (2×)	av <i>d</i> (Na—O)	2.48(1)
Si2—O1	1.622(4) (2×)		
Si2—O3	1.602(4)	O4—O4 ^I	2.301(7)
Si2—O4	1.618(6)	O4—O5	2.809(5)
		O5...O5 ^{II}	3.605(7)
av <i>d</i> (Si—O)	1.609(3)	O5...O5 ^{III}	3.664(7)
av ∠O—Si—O	109(1)°	O5...O6	3.482(7)
		O5...O7	3.407(7)

^a Symmetry codes: I (0, 1/2 - y, z), II (-x, 1/2, 0); III (x, 0, 0).

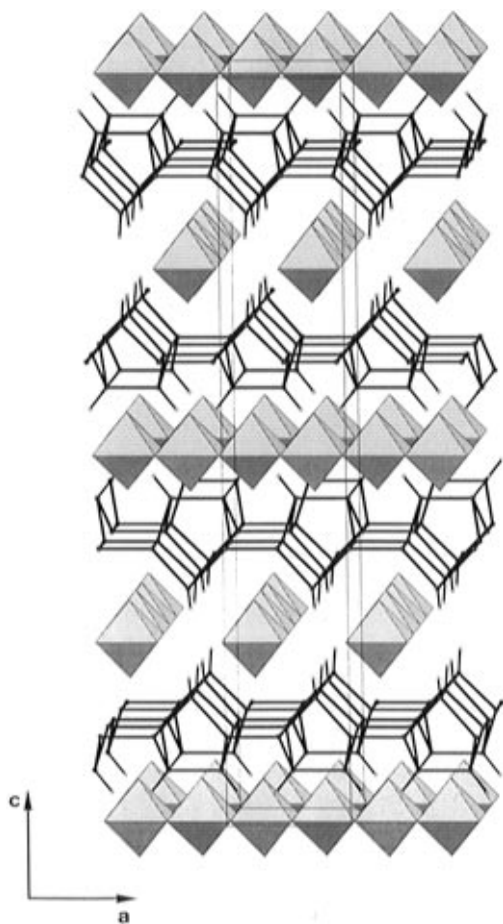


Figure 5. Perspective view of the crystal structure of RUB-18: the silicate layer is represented as skeleton model showing only the silicon atoms and the silanol groups. Bonding oxygen atoms are located in the middle of the Si...Si bonds. The octahedrally coordinated sodium cations form one-dimensional chains of edge-sharing [NaO₆] octahedra.

Results and Discussion

The silicate layer found in RUB-18 has a unique topology. The basic unit is a cage made of four five-membered rings, [5⁴] cages, containing eight [SiO₄] tetrahedra (Figure 7). Each cage is connected with eight oxygen bridges from four silicon atoms symmetrically to four neighboring cages (Figure 6). The remaining four silicon atoms carry the hydroxyl group or the negative charge respectively for the compensation of the charges of the sodium cations. This [5⁴] cage has never been observed in layered silicates, although it is well-known from a number of zeolite structures such as zeolite β, the structure types MFI (e.g., zeolite ZSM-5), MEL (e.g., zeolite ZSM-11), and FER all typical examples for high silica zeolite structures. In addition, the topology of the silicate layer shows close resemblance with the basic layer of zeolite β. In the β-layer

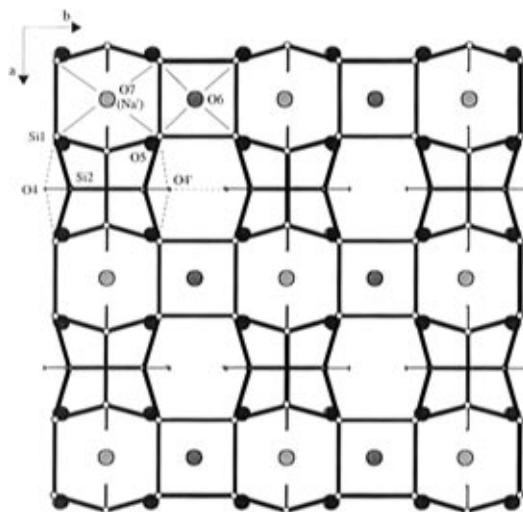


Figure 6. Upper view of the silicate layer at *z* ~ 0.07 and of the sodium chains below: (black circles) basal, (light and dark gray circles) apical water molecules of the sodium octahedra. (In this projection the positions of the sodium cations and of the apical water molecules coincide.) The apical molecules are closer to the sodium cation (2.25 and 2.34 Å) than the basal ones (2.57 Å (4×)).

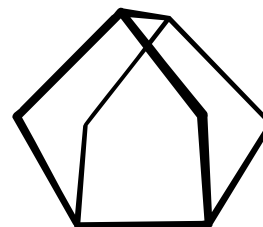


Figure 7. Structural building unit of the silicate layer is the [5⁴] cage, consisting of four five-membered rings. This is the first time that this cage, which is known from several high silica zeolites, is observed in a layered silicate.

neighboring [5⁴] cages are linked through a four-membered ring, leading to a 12-membered ring pore in the layer instead of the six-membered ring pore of RUB-18. Nevertheless, the structure of RUB-18 contains important elements of structures of microporous materials and should be regarded as a precursor structure to the three-dimensional four-connected microporous framework silicates.

The charge-carrying sodium cations reside in the pockets between two silicate layers and are octahedrally coordinated by the oxygen atoms of the intercalated water molecules. The [NaO₆] octahedra share edges to give one-dimensional chains (Figure 5). The nearly regular octahedron explains the narrow resonance signal in the ²³Na NMR spectrum and is linked via hydrogen bridges to the silanol groups of the two adjacent silicate layers (Figure 8). Formally, from a total of 16 silanol groups per unit cell, eight carry a negative charge to compensate the charge of the sodium cations, while the remaining eight still have hydroxyl groups with acidic protons. However, it is most likely that the negative charge is distributed over the hydrogen bond network instead of being localized on particular silanol groups. The result of the structure determination leads to the chemical formula Na₈[Si₃₂O₆₄(OH)₈]·32H₂O for RUB-18, which is in good agreement with the analytical results obtained from complementary experiments.

In the literature, a variety of sodium layer silicates are found, e.g., the minerals kanemite, makatite, magadiite, and kenyaite and the synthetic material ilerite or octosilicate.¹ So far, only the crystal structure of makatite¹⁸ has been solved. This structure, together with model building techniques, X-ray powder data, and ²⁹Si NMR experiments, has served as the basis for deriving model structures for ilerite, magadiite, and kenyaite.

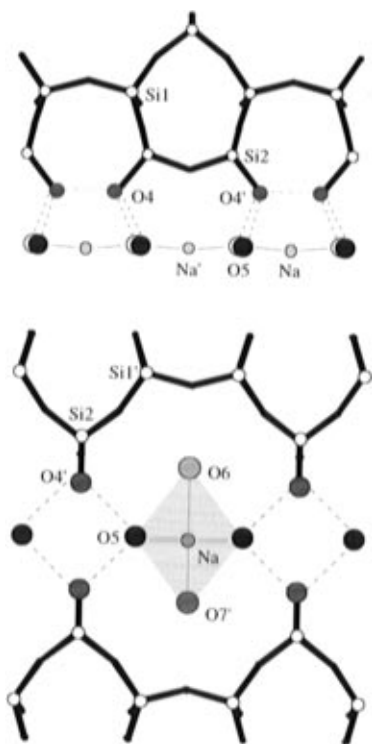


Figure 8. Hydrogen bond network for RUB-18: (a, top) intralayer hydrogen bond between the silanol groups and (b, bottom) hydrogen bond between the silanol groups showing the sp^3 hybridization and the water molecules of the basis of the sodium octahedra.

Although the published powder pattern of ilerite¹⁹ seems to correspond to a sample with a certain degree of preferred orientation and even lower crystallinity, careful inspection of the powder patterns of RUB-18 and ilerite shows remarkable similarity, so that it is most likely that ilerite and RUB-18 are identical materials. Since the proposed model for ilerite is

completely different from the structure found for RUB-18, this model should be discarded if the materials are proved to be the same. One obvious consequence of this result is to question the validity of the remaining two models. In any case, one should be very careful in using model structures if no further evidence from structural work supports them.

Acknowledgment. This work was partially supported by the German DAAD and Spanish DGICYT ("Acción Integrada Hispano-Alemana, 1996–1997").

References and Notes

- (1) Bergk, K. H.; Schwieger, W.; Porsch, M. *Chem. Tech.* **1987**, *11*, 459–504.
- (2) Rius, J.; Miravittles, C. *J. Appl. Crystallogr.* **1988**, *21*, 224–227.
- (3) Gies, H.; Rius, J. *Z. Kristallogr.* **1995**, *210*, 475–480.
- (4) Rius, J. *Acta Crystallogr.* **1993**, *A49*, 406–409.
- (5) Rius, J.; Sanyal, J.; Miravittles, C.; Gies, H.; Marler, B.; Oberhagemann, U. *Acta Crystallogr.* **1995**, *A51*, 840–845.
- (6) Werner, P. E. *Z. Kristallogr.* **1964**, *120*, 375–387.
- (7) Rius, J. AJUST. A whole pattern profile fitting program for extracting integrated intensities; ICMAB-CSIC, Catalunya, Spain, 1995.
- (8) Rius, J. XLENS. A program for crystal structure determination; ICMAB-CSIC, Catalunya, Spain, 1994.
- (9) Baerlocher, Ch.; Hepp, A.; Meier, W. M. DLS-76. A program for the simulation of crystal structures by geometric refinement; ETH Zürich, Switzerland, 1977.
- (10) Siemens Analytical X-Ray Instruments Inc. SHELXTL PC. A program for crystal structure determination, 1990.
- (11) Baerlocher, Ch. ETH, Zürich, 1984.
- (12) Pawley, G. S. *J. Appl. Crystallogr.* **1980**, *13*, 630–633.
- (13) Le Bail, A.; Duroy, H.; Fourquet, J. L. *Mater. Res. Bull.* **1988**, *23*, 447–452.
- (14) Rius, J.; Sañe, J.; Miravittles, C.; Amigó, J. M.; Reventós, M. M.; Lotier, D. *Anal. Quím. Int. Ed.* **1996**, *92*, 223–227.
- (15) David, W. *Nature* **1990**, *346*, 731–734.
- (16) Estermann, M. A.; McCusker, L. B.; Baerlocher, Ch. *J. Appl. Crystallogr.* **1992**, *25*, 539–543.
- (17) Jansen, J.; Peschar, R.; Schenk, H. *J. Appl. Crystallogr.* **1992**, *25*, 237–243.
- (18) Annehed, H.; Fälth, L.; Lincoln, F. J. *Z. Kristallogr.* **1982**, *159*, 203–210.
- (19) Iler, R. K. *J. Colloid Sci.* **1964**, *19*, 648–657.